# Cambridge Centre for Computational Chemical Engineering


## University of Cambridge

Department of Chemical Engineering



Preprint ISSN 1473 – 4273


# Population balance modelling of a droplet size distribution in a RDC: An inverse problem approach


A. Vikhansky, M. Kraft[1], M. Simon, S. Schmidt and H.-J. Bart[2]



submitted: March 1, 2005



[1] Department of Chemical Engineering
University of Cambridge
Pembroke Street
Cambridge CB2 3RA
UK
E-mail: av277@cam.ac.uk, mk306@cam.ac.uk

[2] Department of Mechanical and Process Engineering
Technical University Kaiserslautern
PO Box 3049, 67653 Kaiserslautern
Germany
E-mail: bart@mv.uni-kl.de



Preprint No. 28


**c4e**


*Key words and phrases.* Two-phase systems, sensitivity analysis, inverse problems, Monte Carlo, population balances, weighted particles method.

**Edited by**
Cambridge Centre for Computational Chemical Engineering
Department of Chemical Engineering
University of Cambridge
Cambridge CB2 3RA
United Kingdom.

**Fax:** + 44 (0)1223 334796
**E-Mail:** c4e@cheng.cam.ac.uk
**World Wide Web:** http://www.cheng.cam.ac.uk/c4e/

**Abstract**

An inverse problems method is applied to a two-phase liquid-liquid system in a Rotating Disc Contactor (RDC). The dispersed phase is modelled by population balance equations, which are solved by a Monte Carlo method together with the equations for the parametric derivatives of the solution with respect to the parameters of the model. The best fitting problem is solved by a gradient search method. Since the inverse problem is ill-posed, the iteration procedure is augmented by an appropriate termination criterion to stabilize the calculations. The parametric derivatives of the solution can be used to quantify the relative importance of different parameters of the model. It is shown that the model's parameters, which are identified on one set of the experimental data describe adequately the behavior of the system under another unfitted operation condition, i.e., the proposed method can be applied to scale up problems.

# Contents

# 1 Introduction

The common framework for the description and analysis of two-phase systems consists of mass, momentum and energy balances, which require some additional closure relationships in order to make the equations mathematically tractable. A difficulty arises from the relationship between the available experimental data and the information that is needed for an analytical description of multiphase flows. The experimentally accessible quantities such as gas hold-up or interphase area characterize the dispersed system as a whole, while the mathematical modelling requires more detailed information about single droplet behavior and droplet-droplet interaction. Therefore, an additional mathematical treatment is necessary to extract this information from the measurements, i.e., the solution of the inverse problem is a necessary part of a reliable modelling strategy.

Inverse problems for population balances have attracted much attention in recent years [14, 3, 16, 12, 9, 18]. The solution of inverse problems is often aided by the self-similar behavior of many practically important dispersed systems [14, 9]. In more general cases a mathematical programming procedure has to be applied in order to find the best fit of the experimental data. Note that inverse problems are highly sensitive to errors in the experimental data [19]. Since the experimental results always contain some noise, a regularization scheme has to be implemented to make the numerical algorithm stable.

In the present study we consider liquid-liquid flow in a pilot-scale Rotating Disc Contactor RDC [11]. The parameter fitting problem is solved by a gradient-search algorithm [22], where a Monte Carlo method is used for the solution of the population balance problem and the calculation of the parametric derivatives of the solution. This approach has several important advantages: (i) a Monte Carlo method can easily be extended to a multidimensional case, (ii) gradient search is faster than other methods of mathematical programming, (iii) an efficient regularization scheme, namely, iterative regularization [1] can be used; and (iv) the parametric derivatives indicate which parameters should be identified accurately and which can be postulated approximately because of their weak effect on the simulation results.

# 2 Experimental

The schematic view of the RDC [11] is given in Fig.1. The device is $2200mm$ high (active length is $1500mm$), its internal diameter is $150mm$ and the diameter of the rotating shaft is $D_s = 54mm$. The external diameter of the discs and the internal diameter of the baffles are $D_r = 92mm$ and $D_b = 105mm$, respectively. The extraction system examined is the EFCE-test-system water-toluene [10]. Before each experiment the continuous water phase and the dispersed toluene phase have been mutually saturated. The angular velocity of the shaft $\Omega_s$ varies from $250rpm$ to $450rpm$. The continuous phase which has higher density $\rho_c = 0.998g/cm^3$ and viscosity $\mu_c = 0.92g/(cm\ s)$ is supplied from above with volume flux $Q_c = 50-120l/hr$,

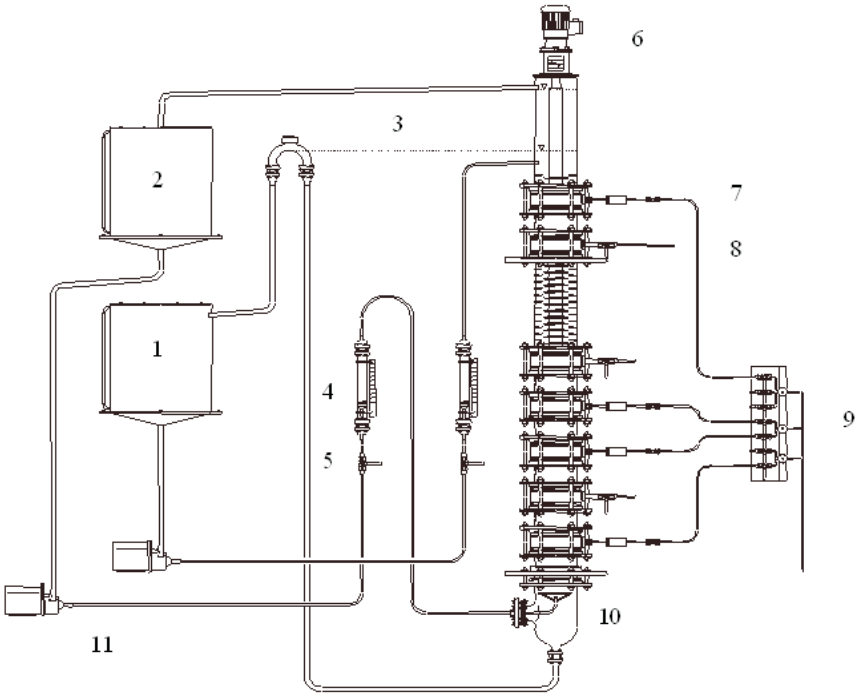


**Figure 1:** *Schematic view of the rotating disc contactor. 1 water reservoir, 2 organic phase reservoir, 3 water overflow, 4 flow meter, 5 valve, 6 motor, 7 droplet sampling tube, 8 valve for hold-up measurement, 10 distributor, 11 pump.*

i.e., the average downward velocity is less than $0.18cm/s$, which is several orders of magnitude less than the local velocities encountered in the system. The dispersed (lighter) phase with density $\rho_d = 0.856g/cm^3$ is supplied through the bottom of the column with volume flux $Q_d = 50 - 120l/hr$. The interphase pressure tension is $\sigma = 36g/s^2$. For varying operational conditions droplet size distributions and hold up values (volume fraction of the dispersed phase) were measured at different column heights. In order to measure the droplet size distributions the established method by Pilhofer and Miller [13] was used. Samples were taken with a photoelectrical capillary suction probe. The hold up of the dispersed phase was determined locally by the direct sampling method.

Initially, the volume of the droplets is distributed according to a cumulative distribution function $F_{in}(v)$, as the droplets move through the RDC, the distribution changes due to coalescence and breakage. Due to the rotation of the discs the fluid is centrifuged outward in the radial direction and after impinging on the outer wall is reflected inwards and forms voricity cells in each compartment [21]. The droplets rise up but are trapped by the vorticity in each compartment which play the role of partially mixed reactors.

The power input in one compartment, $P$, is given by [11]:

$$P = 8.48 Re_r^{-0.4} \Omega_s^3 D_r^5,$$

where $Re_r$ is the Reynolds number of the rotor:

$$Re_r = \frac{\rho_c D_r^2 \Omega_s}{\mu_c}.$$

The number density of the droplets of diameter $a$ at time $t$ is $n(t,a)$ and the volume fraction of the droplets of diameter $a$ to $a+da$ is $\phi(t,a)da = an(t,a)da$, while the total volume fraction of the droplets in a compartment is $\Phi(t) = \int_0^\infty \phi(t,\xi)d\xi$. Then the equation of population balance of droplet size distribution in a compartment reads

$$\frac{\partial \phi(t,a,c)}{\partial t} = B(\phi,c) - D(\phi,c), \tag{1}$$

where $B$ and $D$ represent birth and death of the droplets respectively. The unknown (generally speaking, vector) parameter $c$ has to be extracted from the experimental data. In the present investigation we assume that the system is in steady state and the RDC is long enough to neglect the inlet/outlet effects. The observations show that initially the characteristic size of the droplets decreases due to the breakage when the droplets rise up, but in the central part of the RDC the breakage and coalescence are mutually balanced. All the measurements presented in this article are done in the $104^{th}$ compartment (out of 176) of the RDC. Thus we apply to this compartment the periodic boundary conditions, that is, the compartment above and below the given one have the same droplet size distributions.

# 3 Two phase hydrodynamics model: breakage, coalescence and transport

According to the common view on the fragmentation of bubbles and droplets in turbulent flows, a droplet breaks if the dynamic pressure due to the turbulence exceeds the pressure due to the surface tension, while the mechanisms that govern the size distribution of the resulting daughter droplets are less clear. The surface pressure of a drop with diameter $a$ is $\tau_s(a) = 6\sigma/a$. The dynamic pressure of the turbulence at the scale of the drop $\tau_t(a)$ is exponentially distributed with parameter

$$\bar{\tau}_t = \frac{1}{2}\rho_c \overline{\Delta u^2(a)} = \frac{1}{2}\beta \rho_c (\varepsilon a)^{2/3},$$

where $\overline{\Delta u^2(a)}$ is the characteristic velocity difference between two points separated by distance $a$, the constant $\beta = 8.2$ was given by Batchelor [2] and $\varepsilon$ is the dissipation rate of the turbulence which is the power input $P$ divided by the volume of the compartment. The fraction of eddies with a dynamic pressure greater than $\tau_s(a)$ is

$$\int_{\tau_s(a)}^\infty \exp\left(-\frac{\tau}{\bar{\tau}_t}\right) d\frac{\tau}{\bar{\tau}_t} = \exp\left(-\frac{\tau_s(a)}{\bar{\tau}_t}\right). \tag{2}$$

The time that is necessary for breakage can be estimated as the life time of the turbulent vortex with size $a$:

$$\frac{1}{t_{break}} = \frac{\sqrt{\overline{\Delta u^2(a)}}}{a} = \sqrt{\beta}\frac{\varepsilon^{1/3}}{a^{2/3}}. \tag{3}$$

Combining of Eqs. (2) and (3) yields the following formula for the droplets breakage rate [4]:

$$c_1\sqrt{\beta}\frac{\varepsilon^{1/3}}{a^{2/3}}\exp\left(-c_2\frac{\sigma}{\beta\rho_c\varepsilon^{2/3}a^{5/3}}\right), \tag{4}$$

where $c_1$, $c_2$ are empirical constants which have to be identified.

Although the general mechanisms of droplets breakage in a turbulent flow are known, less information is available about the size distribution of the daughter droplets formed upon breakage. In the present investigation we have assumed that a droplet with volume $v$ breaks into two droplets with volumes $v'$ and $v-v'$, respectively. The volume $v'$ of the daughter droplet is generated as

$$v' = \frac{v}{\pi}\arccos(1-2\gamma),$$

where $0 \leqslant \gamma \leqslant 1$ is a uniformly distributed random variable. Note, that more sophisticated breakage models which can be found in the literature (see, e.g., [20] and references therein) contain more empirical constants and, therefore, require a larger amount of the experimental data to identify them.

The coalescence rate of two droplets with volumes and diameters $v_1$, $v_2$, $a_1$ and $a_2$, respectively, has been described in [4] as the product of the collision frequency $h_{1,2}$ and efficiency of the collision $\lambda_{1,2}$. The relations for $h_{1,2}$ and $\lambda_{1,2}$ are:

$$h_{1,2} = c_3\frac{\varepsilon^{1/3}}{1+\Phi}(v_1^{1/3}+v_2^{1/3})^2(v_1^{2/9}+v_2^{2/9})^{1/2}.$$

$$\lambda_{1,2} = \exp\left\{-c_4\frac{\mu_c\rho_c\varepsilon}{\sigma^2(1+\Phi)^3}\left(\frac{a_1a_2}{a_1+a_2}\right)^2\right\}.$$

The residence time of a droplet of size $a$ in the compartment is

$$\tau_{res}(a) = \frac{h_c}{v(a)},$$

where $h_c$ is the height of the compartment and $v(a)$ is the rising velocity. The rising velocity is the sum of the relative velocity of the droplet with respect to the continuous phase $v_r(a)$ and the (downward directed) velocity of the continuous phase $v_c$:

$$v(a) = v_r(a) + v_c = v_r(a) - \frac{Q_c}{A(1-\Phi)},$$

where $A$ is the cross section of the column.

Different correlations have been proposed to model the rising velocity of the droplets in extraction columns (see, e.g., [7, 6] and references therein). The general approach is to relate $v_r(a)$ to the terminal velocity of a single droplet $v_T(a)$:

$$v_r(a) = k_v v_T(a),$$

where $k_v$ is a slowing factor which takes into account the effects of the column's internals and flow structures inside the compartments. Generally speaking, $k_v$ is a function of column geometry, void fraction of the dispersed phase and the rotation velocity of the shaft. The empirical correlations for $k_v$ available in the literature contain a large number $(5-6)$ of empirical parameters. Our numerical experiments show that the available amount of experimental data does not allow for reliable identification of so many parameters. On the other hand, a much simpler model, namely, constant slowing factor

$$k_v = c_5$$

satisfactorily approximates the experimental results for the whole range of the operational conditions.

The correlation which we used for $v_T(a)$ reads [11]:

$$v_T(a) = \frac{a}{4.2}\left(g\frac{\rho_c - \rho_d}{\rho_c}\right)^{2/3}\left(\frac{\rho_c}{\mu_c}\right)^{1/3}\left(1 - \frac{E\ddot{e}}{6}\right),$$

where $E\ddot{e}$ is the Eëtvös number:

$$E\ddot{e} = \frac{ga^2(\rho_c - \rho_d)}{\sigma}.$$

# 4 Parameter identification

The purpose of the present work is not only to fit the experimental results, but also to check whether the fitted model can predict the dynamics of the system under another, unfitted conditions. In order to achieve this task we divided the experiments, with operation conditions presented in Table 1, into two groups. Experiments (a) - (c) with relatively low flow rate of the dispersed phase were used to identify the parameters $c_i$ of the model and then the fitted model was applied to scale the system up, namely, to predict the outcome of the experiments (d) - (f) as displayed in Fig. 3, which have higher flow rate. Note that in the steady state, multiplication of the breakage and collision pre-exponential factors $c_1$ and $c_2$ by the same constant does not change the solution. Thus in the present work we assume that $c_1 = 2.0 \cdot 10^{-2}$ (a value similar to those recommended in the literature) and identify only four parameters $c_2$, ...$c_5$. In each experiment the dispersed phase volume fraction and number size distribution function are measured. Since the available experimental data is quite noisy, we use it to calculate several first *mass*-averaged moments, which are less affected by the experimental error. The expression for the $j^{th}$ moment obtained

**Table 1:** *Operational conditions of RDC.*

| Experiment | $\Omega_s$ (RPM) | $Q_d$ $(l/h)$ | $Q_c$ $(l/h)$ |
|---|---|---|---|
| a) | 300 | 56 | 100 |
| b) | 350 | 56 | 100 |
| c) | 450 | 56 | 100 |
| d) | 250 | 120 | 100 |
| e) | 300 | 112 | 50 |
| f) | 350 | 120 | 100 |

in the $i^{th}$ experiment reads:

$$D_{ij} = \int \phi_i(a) a^j da = \frac{\pi}{6} \int n_i(a) a^{(j+3)} da, \;\; j = 0, ..., 3.$$

Then we solve an identification procedure, i.e., look for the set of parameters $\vec{c^*} = (c_2^*, ...c_5^*)$ that minimizes the residual between the predicted and the experimental results:

$$\Theta = \frac{1}{2} \sum_{i=1,j=0}^{3} \varrho_j \left( \frac{D_{ij}(\vec{c}) - D_{ij}^{exp}}{D_{ij}^{exp}} \right)^2, \tag{5}$$

where $\varrho_j = 1/2^j$ is an empirical weighting factor, i.e., hold-up has to be fitted more accurately than the dispersion of the diameter.

We solve problem (5) by a quasi-Newtonian algorithm, where a Monte Carlo method is used for the solution of Eq. (1) and the calculation of the gradients $\partial\phi/\partial c$. The details of the algorithm [22] are given in the Appendix. As soon as the parametric derivatives are known, an efficient quasi-Newtonian method can be applied to the minimization of the residual (5). We use the following minimization algorithm, at each iteration $\vec{c}$ is represented as $\vec{c} + \Delta\vec{c}$. Since the parameters $c_i$ have different orders of magnitude, we rescale the increments of the parameters as $\Delta c_i = c_i \beta_i$, where $\beta \sim 1$. Then we expand the moments $D_{ij}$ as $D_{ij}(\vec{c}) = D_{ij}(\vec{c}) + \beta_l c_l \partial_{c_l} D_i(\vec{c})$. Substitution of this formula into (5) and differentiation with respect to $\vec{\beta}$ yields the following system of linear algebraic equations with respect to the relative increment $\vec{\beta}$:

$$A\vec{\beta} = \vec{b}, \tag{6}$$

where

$$a_{lm} = \sum_{i=1,j=0}^{3} \varrho_j \left( \frac{\partial D_{ij}}{\partial c_l} \frac{\partial D_{ij}}{\partial c_m} \right) \frac{c_l c_m}{(D_{ij}^{exp})^2} \tag{7}$$

and

$$b_l = \sum_{i=1,j=0}^{3} \varrho_j c_l \frac{D_{ij}^{exp} - D_{ij}(\vec{c})}{(D_{ij}^{exp})^2} \frac{\partial D_{ij}}{\partial c_l}. \tag{8}$$

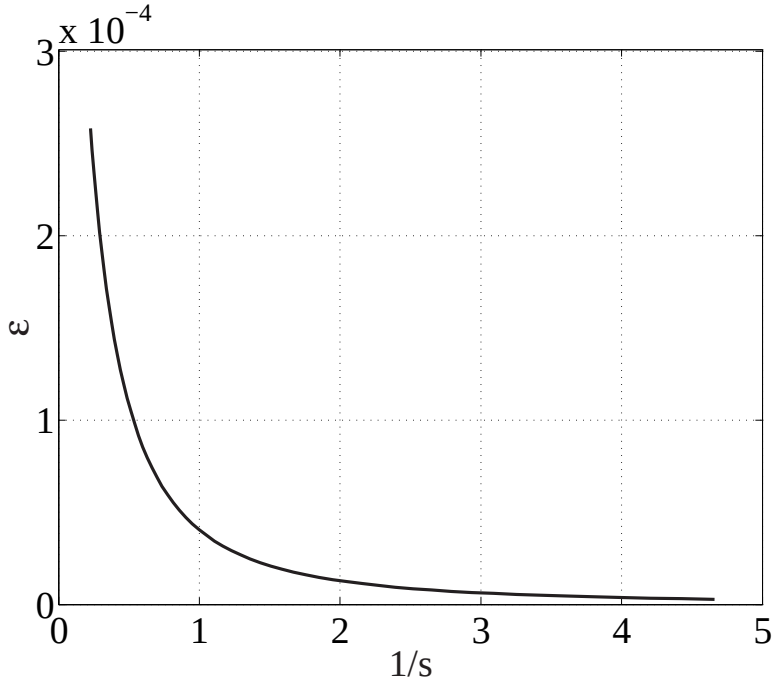


**Figure 2:** *Example of the error of the solution of Eq. (6) as function of the regularization parameter.*

One can see that the vector $\vec{b}$ is nothing else but the gradient of the residual $\Theta$ with respect to $\beta$.

Note, that the matrix $A$ is badly scaled, thus we regularize Eq. (6) as

$$(sE + A)\vec{\beta} = \vec{b}, \tag{9}$$

where $s$ is a parameter of regularization and $E$ is an unit matrix. If we plot the error due to the regularization $\varepsilon = (A\vec{\beta} - \vec{b})^2$ as a function of $1/s$ (see Fig. 2), we can see that the error is low for high $s$ and has a characteristic bend for some value of $s$. The region of the bend gives a good compromise between the stability and the precision of the computations. If the parameter of regularization $s$ is very high, the method, described above, becomes a gradient search method with fixed step.

The difference $\left(D_{ij}^{exp} - D_{ij}\right)$ in Eq. (8) contains two types of error. One is the systematic error because the model is an approximate one and cannot reproduce the experimental results exactly. The second error is due to the unavoidable experimental noise which is very strong in every dispersed system. Since we use a Monte Carlo method for the solution of Eq. (1), the computed moments $D_{ij}$ also contain some error. Initially, when the systematic error is larger than the statistical, the direction of the steepest descend $\vec{b} = \nabla\Theta$ is insensitive to the random noise. Therefore, during the first few iterations of the minimization algorithm the identified parameters approach the exact values, i.e., those values which they would have in the "no noise" case. As the residual decreases, the random component has higher

**Table 2:** *Identified parameters and residuals.*

| No. of iteration | $c_2$ | $c_3$ | $c_4$ | $c_5$ | $\Theta$ | $\|\nabla\Theta\|$ |
|---|---|---|---|---|---|---|
| 0 | 10.0 | 2.00e-2 | 1.00e3 | 0.300 | 1.85e-1 | 2.93e-1 |
| 1 | 6.87 | 1.43e-2 | 1.16e3 | 0.260 | 8.14e-2 | 2.18e-1 |
| 2 | 8.08 | 1.29e-2 | 1.29e3 | 0.268 | 6.24e-2 | 3.40e-2 |
| 3 | 9.10 | 1.17e-2 | 1.63e3 | 0.264 | 6.12e-2 | 3.29e-2 |

relative contribution to (8). Since the random components of $D_{ij}^{exp}$ mutually cancel during the summation over $i$ and $j$, the gradient $\nabla\Theta$ becomes very small. Thus, the identified parameters start to recede from the exact ones while the residual does not decrease significantly. At this point the calculations have to be terminated to avoid instability [1].

The results of the calculations which are presented in Table 2 illustrate this process. During the first two iterations, the residual decreases quickly, while at the third iteration the gradient $\nabla\Theta$ sharply decreases and the significant change of the parameters $c_i$ does not improve the solution. Therefore, we can identify the second iteration as the beginning of the instability and terminate the iterations here.
The calculated and measured droplets size distributions are presented in Fig. 3. As we can see, the results of the computations approximate both the the fitted and the unfitted experimental data with a satisfactory precision. To quantify the difference between the experimental and the numerical results we calculated the most important characteristics of the dispersed system, namely, the volume fraction of the droplets $\Phi$, their mass-mean diameter

$$d_m = \Phi^{-1} \int \phi(a) da$$

and Sauter mean diameter

$$d_s = \frac{\int n(a) a^3 da}{\int n(a) a^2 da},$$

which are presented in Table 3. The relative difference $\epsilon_\vartheta$ between the experimental and the numerical values of a feature $\vartheta$ is

$$\epsilon_\vartheta = \frac{\vartheta_{num} - \vartheta_{exp}}{\vartheta_{exp}}.$$

The relative error does not exceed 20%, the only exception is the experiment $(e)$. As one can see, the experimentally obtained volume density functions contain some noise. From general considerations we would expect that a higher agitation rate increases the volume fraction of the dispersed phase (one can compare the experiments $(a)$-$(c)$), while $\Phi$ registered in the experiment $(e)$ is lower than in $(d)$, which corresponds to the lower angular velocity of the shaft. Thus, we assume that part of the error is due to the experimental noise, which is unavoidable in two-phase systems.

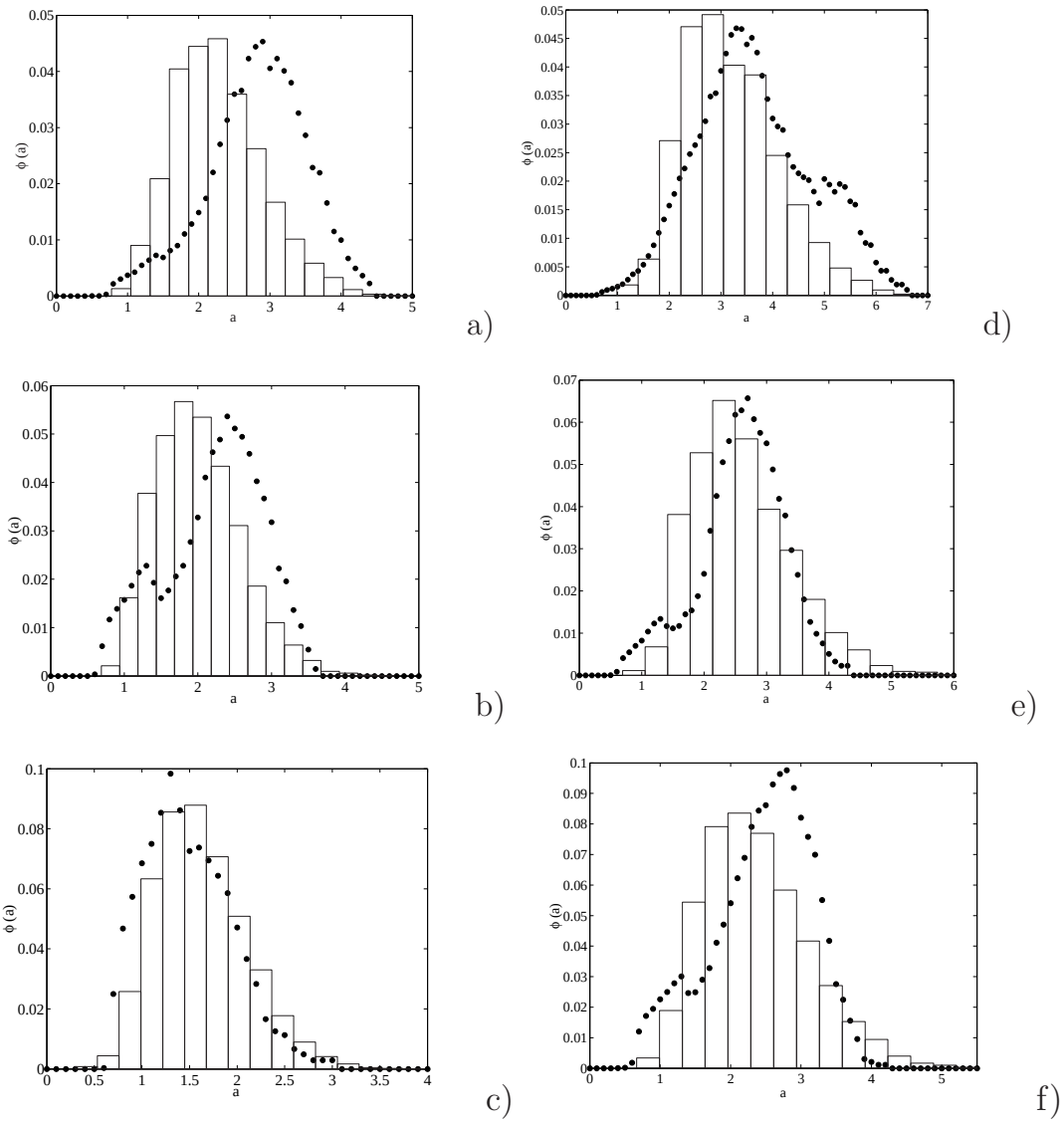


**Figure 3:** *Fitted (left column) and unfitted (right column) numerical (histograms) and experimental (points) volume density functions $\phi(a)$ $(mm^{-1})$ as function of the diameter (mm). The operational conditions are given in Table 1.*

**Table 3:** *Comparison of the experimental and the numerical results.*

| Exp. | $\Phi_{num}$ | $\Phi_{exp}$ | $\epsilon_\Phi$ (%) | $d_{m_{num}}$ | $d_{m_{exp}}$ | $\epsilon_{d_s}$ | $d_{s_{num}}$ | $d_{m_{exp}}$ | $\epsilon_{d_s}$ (%) |
|---|---|---|---|---|---|---|---|---|---|
| a) | 0.0709 | 0.072 | -1.5 | 2.28 | 2.77 | -18 | 2.11 | 2.60 | -19 |
| b) | 0.0824 | 0.0787 | 5.0 | 2.00 | 2.18 | -8.3 | 1.84 | 1.97 | -6.6 |
| c) | 0.104 | 0.105 | -0.95 | 1.62 | 1.44 | 13 | 1.48 | 1.37 | 8.0 |
| d) | 0.111 | 0.116 | -4.3 | 3.20 | 3.60 | -11 | 2.95 | 3.26 | -9.5 |
| e) | 0.118 | 0.0956 | 23.0 | 2.60 | 2.55 | 2.0 | 2.37 | 2.50 | -5.2 |
| f) | 0.154 | 0.158 | -2.5 | 2.37 | 2.37 | -1.3 | 2.15 | 2.16 | -0.46 |

It is obvious that different empirical parameters have different effects on the solution of Eq. (5). Those parameters which have a weak effect on the output of the computations cannot be identified with reasonable precision. On the other hand these parameters do not have to be known accurately. The sensitivity analysis gives an opportunity to identify the important and unimportant parameters and combinations of them. To proceed further let us expand the residual $\Theta$ in the vicinity of the optimal set of parameters $c_i^*$ into Taylor series:

$$\Theta(\vec{c}) \approx \Theta(\vec{c}^*) + \frac{1}{2}(\vec{c} - \vec{c}^*)^T A(\vec{c} - \vec{c}^*).$$

The matrix $U$ of eigenvectors $\vec{u}_i$ and the vector of corresponding eigenvalues $\lambda_i$ of the matrix $A$ are

$$U = \begin{pmatrix} 0.0577 & -0.7862 & 0.6138 & -0.0433 \\ 0.0448 & -0.6015 & -0.7570 & 0.2513 \\ -0.0035 & 0.1215 & 0.2242 & 0.9669 \\ 0.9973 & 0.0730 & -0.0007 & -0.0053 \end{pmatrix} \tag{10}$$

and

$$\vec{\lambda}^T = \begin{pmatrix} 9.68 & 1.65 & 9.89\text{e-}3 & 3.79\text{e-}4 \end{pmatrix}, \tag{11}$$

respectively. If we denote the uncertainty of the residual as $\Delta\Theta$, the uncertainty of the identified parameters in the direction of the eigenvector $\vec{u}_i$ can be estimated as $\Delta\vec{c} \approx (\Delta\Theta/\lambda)^{1/2}\vec{u}_i$. As follows from Table 2, $\Delta\Theta$ can be estimated as $\Delta\Theta \approx 10^{-2}$ and $\Delta\vec{c}$ along the third and the forth eigenvectors is about 100% and 500%, respectively. The third and forth columns of matrix $U$ show that, while the slowing factor $k_v = c_5$ can be identified with reasonable precision, simultaneous increase/decrease of collision and coalescence rates or, alternatively, increase/decrease of the pre-exponential factor $c_3$ and the exponential coefficient $c_4$ do not change the results of the computations significantly.

To quantify the effect of different parameters on the solution of Eq. (5) we define the coefficient of sensitivity $S^{\vartheta}_{c_i}$ of a feature $\vartheta$ to the coefficient $c_i$ as the ratio of the relative change of $\vartheta$ to the relative change of $c_i$:

$$S^{\vartheta}_{c_i} = \frac{\Delta \ln \vartheta}{\Delta \ln c_i}.$$

**Table 4:** *Sensitivities of the volume fraction of the dispersed phase, $\Phi$, with respect to the corresponding parameters.*

| Exp. | $c_1$ | $c_2$ | $c_3$ | $c_4$ | $c_5$ |
|---|---|---|---|---|---|
| a) | 0.1655 | -0.3814 | -0.1661 | 0.0353 | -0.9668 |
| b) | 0.2011 | -0.4602 | -0.2063 | 0.0472 | -0.9381 |
| c) | 0.2133 | -0.4230 | -0.2387 | 0.0681 | -0.9638 |
| d) | 0.1622 | -0.3020 | -0.1533 | 0.0368 | -0.9675 |
| e) | 0.1951 | -0.3790 | -0.2052 | 0.0516 | -0.8884 |
| f) | 0.2418 | -0.4338 | -0.2354 | 0.0665 | -0.9338 |

**Table 5:** *Sensitivities of mass-mean diameters, $d_m$, with respect to the corresponding parameters.*

| Exp. | $c_1$ | $c_2$ | $c_3$ | $c_4$ | $c_5$ |
|---|---|---|---|---|---|
| a) | -0.1580 | 0.3629 | 0.1657 | -0.0356 | -0.2063 |
| b) | -0.1833 | 0.4040 | 0.1971 | -0.0469 | -0.2259 |
| c) | -0.2020 | 0.4279 | 0.1958 | -0.0552 | -0.2534 |
| d) | -0.1870 | 0.3331 | 0.1779 | -0.0438 | -0.2054 |
| e) | -0.2368 | 0.4431 | 0.2164 | -0.0568 | -0.1992 |
| f) | -0.2230 | 0.3902 | 0.2171 | -0.0617 | -0.2604 |

**Table 6:** *Sensitivities of Sauter mean diameters, $d_s$, with respect to the corresponding parameters.*

| Exp. | $c_1$ | $c_2$ | $c_3$ | $c_4$ | $c_5$ |
|---|---|---|---|---|---|
| a) | 2.0210 | -4.5994 | -2.0253 | 0.4342 | -12.8457 |
| b) | 2.0745 | -4.7045 | -2.1192 | 0.4896 | -10.6512 |
| c) | 1.6482 | -3.1708 | -1.8679 | 0.5426 | -8.4998 |
| d) | 1.1224 | -2.0520 | -1.0725 | 0.2612 | -7.9546 |
| e) | 1.2465 | -2.3719 | -1.3462 | 0.3435 | -6.8062 |
| f) | 1.1236 | -1.9540 | -1.0990 | 0.3193 | -5.3549 |

The sensitivity coefficients for the volume fraction of the dispersed phase, mass-mean diameter and Sauter mean diameter are given in Tables 4-6. The signs of the computed sensitivity coefficients are intuitively clear: breakage decreases the mean diameter of the droplets and increases the interphase area. Since smaller droplets have lower terminal velocities, intensive breakage increases the volume fraction of the dispersed phase. The effect of coalescence is opposite to the effect of breakage. One can also see that the exponential coefficient $c_4$ has significantly lower effect than other parameters of the model and this coefficient has not to be identified with high precision.

# 5 Conclusions

A Monte Carlo method was applied to a droplet's population balance in two-phase liquid-liquid flow. The method allows for the calculation of the derivatives of the solution with respect to the empirical coefficients of the model. As soon as the parametric derivatives are known an efficient gradient search method can be used to minimize the difference between the observed and the numerical results, i.e., the unknown empirical parameters of the model can be extracted from the available experimental data. Iterative regularization [1] was used to stabilize the solution of the inverse problem. Only a few iterations of the gradient algorithm are required to identify the unknown coefficients. The coefficients identified on the basis of one set of experimental data can be used to predict the behavior of the system under different operation conditions. The proposed methods also provides information about sensitivity of the solution to the parameters of the model, this information can be used to decide which parameters have to be identified with high precision.

# Acknowledgement

This work has been supported by the EPSRC (grant number GR/R85662/01) under the title "Mathematical and Numerical Analysis of Coagulation-Diffusion Processes in Chemical Engineering".

# A Calculation of parametric derivatives of the solution of the population balance equation

To illustrate the method for calculations of parametric derivatives of the solution of the population balance equation, consider for simplicity the space-homogeneous

Smoluchowski coagulation equation

$$\frac{\partial n(t,x;\lambda)}{\partial t} = \frac{1}{2}\int_0^x K(x-x',x';\lambda)n(t,x-x';\lambda)n(t,x';\lambda)dx' - \int_0^\infty K(x,x';\lambda)n(t,x;\lambda)n(t,x';\lambda)dx', \tag{A.1}$$

where $n(t,x;\lambda)$ is the number density of particles that have mass $x$ at the time $t$. The probability that two particles with masses $x$ and $x'$, respectively, coalesce during a small time interval $dt$ is $K(x,x';\lambda)dt$, where $\lambda$ is a parameter. In order to proceed further let us reformulate Eq. (A.1) in terms of mass density. The advantages of this formulation are discussed in [5, 8], note also, that particle mass distributions encountered in technological applications more frequently than number distributions [15, 14]. The mass density of the particles that have mass $x$ at a time $t$ is $m(t,x) = xn(t,x)$. The total mass of the system is $M = \int mdx$. In order to rewrite the coagulation equation (A.1) in terms of mass density, we express $n(t,x)$ as $m(t,x)/x$, substitute it into (A.1) and multiply the equation by $x$. Note, that if $K(x,x') = 0$ for $x \leqslant 0$ or $x' \leqslant 0$, the limits of integration in (A.1) can be extended from $-\infty$ to $\infty$. After some algebra we obtain [14, 5]:

$$\frac{\partial m(t,x;\lambda)}{\partial t} = \int \frac{K(x-x',x';\lambda)}{x'} m(t,x-x';\lambda)m(t,x';\lambda)dx' - \int \frac{K(x,x';\lambda)}{x'} m(t,x;\lambda)m(t,x';\lambda)dx'. \tag{A.2}$$

The factor of $1/2$ before the first integral in Eq. (A.2) disappears because coagulation reduces the number of particles but does not affect their mass.

Consider a stochastic particle system

$$x_1(t), ..., x_N(t),$$

which approximates the mass density function $m(t,x)$ as

$$m(t,x) \approx \sum_{n=1}^{N} w_n \delta(x - x_n(t)), \tag{A.3}$$

i.e., each particle in the above $N$-particle system represents a group of identical physical particles with size $x_n$. The total mass of the $n^{th}$ group is $w_n$ and the number of particles in the group is $w_n/x_n$. Since the probability that during a small time interval $dt$ the $k^{th}$ particle will coagulate with one particle from the $l^{th}$ group is $K(x_k,x_l;\lambda)dt$, the probability that the $k^{th}$ particle will coagulate with any of the $l^{th}$ particles is

$$\pi_{kl}(\lambda)dt = \frac{K(x_k,x_l;\lambda)w_l}{x_l}dt.$$

Thus, the coagulation rate of the $k^{th}$ particle is given by the summation of the above formula over $l$. The formula for the total collision rate reads:

$$\sum_{\alpha=1,\beta=1}^{N} \pi_{\alpha\beta}(\lambda), \tag{A.4}$$

and the collision pair is chosen with the relative probability

$$\frac{\pi_{kl}(\lambda)}{\sum_{\alpha=1,\beta=1}^{N}\pi_{\alpha\beta}(\lambda)}. \tag{A.5}$$

In the present investigation we use the acceptance-rejection technique similar to that used in [5]. Let us consider a majorant kernel and majorant weights satisfying

$$K(x_k, x_l; \lambda) \leqslant \hat{K}(x_k, x_l),\ w_l \leqslant \hat{w}_l,\ \pi_{kl}(\lambda) \leqslant \hat{\pi}_{kl} = \hat{K}(x_k, x_l)\hat{w}_l.$$

The corresponding stochastic algorithm reads:

1. Generate an exponentially distributed time increment $\tau$ with parameter

$$\sum_{\alpha=1,\beta=1}^{N}\hat{\pi}_{\alpha\beta}; \tag{A.6}$$

2. Choose a pair $(k, l)$ to collide according to the distribution

$$\frac{\hat{\pi}_{kl}}{\sum_{\alpha=1,\beta=1}^{N}\hat{\pi}_{\alpha\beta}}; \tag{A.7}$$

3. Accept the coagulation with probability

$$\frac{\pi_{kl}(\lambda)}{\hat{\pi}_{kl}}; \tag{A.8}$$

   i.e., $x_k$ is replaced by $x_k + x_l$;

4. Or reject the coagulation and perform a *fictitious* jump that does not change the size of the colliding particles with probability

$$1 - \frac{\pi_{kl}(\lambda)}{\hat{\pi}_{kl}}. \tag{A.9}$$

Notably, the number of particles in this algorithm does not change during the calculations. The particle ensemble at time $t$ is an approximation of the mass density function $m(t, x)$.

Now, consider a functional of the solution of Eq. (A.2):

$$H(t, m; \lambda) = \int m(t, x; \lambda)h(x)dx,$$

where $h(x)$ is an integrable function of $x$. Substitution of Eq. (A.3) into the above equation gives a Monte Carlo estimate of the functional $H$ that is averaged over the $N$-particle ensemble:

$$H(t, m; \lambda) \approx \sum_{n=1}^{N} w_n h(x_n(t)). \tag{A.10}$$

Let us consider the following formula:

$$H(t,m;\lambda+\Delta\lambda)\approx\sum_{n=1}^{N}w_n(1+\Delta\lambda W_n)h(x_n(t)). \tag{A.11}$$

Comparison with Eq. (A.10) reveals that

$$\frac{\partial H(t,m;\lambda)}{\partial\lambda}\approx\sum_{n=1}^{N}w_nW_nh(x_n(t)) \tag{A.12}$$

and

$$\frac{\partial m(t,x;\lambda)}{\partial\lambda}\approx\sum_{n=1}^{N}w_nW_n\delta(x-x_n(t)). \tag{A.13}$$

The above formula can be interpreted as a parametric derivative (in weak sense) of the solution of Eq. (A.2), and $W_n=(\partial_\lambda w_n)/w_n=\partial_\lambda\ln w_n$.
We will refer to a system with weights $w_n(1+\Delta\lambda W_n)$, kernel $K(x_k,x_l;\lambda+\Delta\lambda)$ and

$$\pi_{kl}(\lambda+\Delta\lambda)=\frac{K(x_k,x_l;\lambda+\Delta\lambda)w_n(1+\Delta\lambda W_n)}{x_l}$$

as the "*disturbed* " system, while the original system is referred as an "*undisturbed*" system. The time evolution of the disturbed system is as follows. Since Eqs. (A.6) - (A.7) do not depend on $\lambda$, the only difference between the disturbed and undisturbed systems is at the acceptance-rejection step. The coagulation is accepted with probability

$$\frac{\pi_{kl}(\lambda+\Delta\lambda)}{\hat{\pi}_{kl}}, \tag{A.14}$$

or rejected with probability

$$1-\frac{\pi_{kl}(\lambda+\Delta\lambda)}{\hat{\pi}_{kl}}. \tag{A.15}$$

After this step the average contribution of the $k^{th}$ particle to the functional (A.11) reads:

$$h(x_k+x_l)w_k(1+\Delta\lambda W_k)\times\frac{\pi_{kl}(\lambda+\Delta\lambda)}{\hat{\pi}_{kl}}+$$
$$h(x_k)w_k(1+\Delta\lambda W_k)\times(1-\frac{\pi_{kl}(\lambda+\Delta\lambda)}{\hat{\pi}_{kl}}).$$

Expanding the above formula with respect to $\Delta\lambda$ and keeping the terms up to $O(\Delta\lambda)$ one obtains the average contribution of the $k^{th}$ particle to the functional $H$:

$$h(x_k+x_l)w_k(1+\Delta\lambda(W_k+\partial_\lambda\ln\pi))\times\frac{\pi_{kl}(\lambda)}{\hat{\pi}_{kl}}+$$
$$h(x_k)w_k(1+\Delta\lambda(W_k-\pi\frac{\partial_\lambda\ln\pi}{\hat{\pi}-\pi}))\times(1-\frac{\pi_{kl}(\lambda)}{\hat{\pi}_{kl}}).$$

Comparison of the above formula with Eqs. (A.8)-(A.9) shows that the probabilities of acceptance and rejection in the disturbed system can be the same as in the undisturbed one, i.e., initially all factors $W_k = 0$, the system evolves along the trajectory of the undisturbed system, while at each step (fictitious and non-fictitious) the factors $W_k$ have to be recalculated as

$$W_k = W_k + \partial_\lambda \ln(\pi_{kl}) = W_k + \partial_\lambda \ln(K) + W_l, \tag{A.16}$$

if the coagulation is accepted, or as

$$W_k = W_k - \pi_{kl} \frac{\partial_\lambda \ln \pi_{kl}}{\hat{\pi}_{kl} - \pi_{kl}} = W_k - w_l K \frac{\partial_\lambda \ln(K) + W_l}{\hat{w}_l \hat{K} - w_l K}, \tag{A.17}$$

if the coagulation is rejected. If the particle undergoes breakage or any other process which (unlike coalescence) involves only one particle, the similar considerations yield the following formula for recalculation of $W_k$. Let $g(\lambda)$ be the breakage rate and $\hat{g} \geqslant g(\lambda)$ be a majorant. Then we accept the breakage with the probability $g(\lambda)/\hat{g}$ and recalculate the factor $W_k$ as

$$W_k = W_k + \partial_\lambda \ln(g(\lambda)), \tag{A.18}$$

or reject it with the probability $1 - g(\lambda)/\hat{g}$ and recalculate the factor $W_k$ as

$$W_k = W_k + \partial_\lambda \ln(1 - g(\lambda)/\hat{g}) \tag{A.19}$$

This method for sensitivity analysis of population balance equations has been tested in our previous work [22] and it was shown that the estimation of the parametric derivatives based on Eqs. (A.16), (A.17) has high dispersion. To understand the origin of this dispersion it is enough to note that two identical particles with factors $W$ and $-W$, respectively, give zero contribution to the parametric derivative for any (high) value of $W$. The numerical experiments show that the factors $W$ can grow infinitely which leads to unbounded dispersion of the calculated derivatives. In order to reduce the dispersion we used an weighted particles algorithm which creates one additional particle after each collision, then we used a clustering method [17] to reduce the number of particles.

In the present investigation we use an alternative method which does not require the time-consuming clustering procedure. Assume that we do not need to calculate the parametric derivative of the solution $\partial m(x)/\partial\lambda$ but only derivatives of some first moments of the particle size distribution: total mass, mean diameter, etc. Define a set of functions $h_0(x)$, $h_1(x)$,... $h_K(x)$ (for example, $h_k(x) = x^{k/3}$). Substitution of these functions into Eq. (A.12) yields a system of linear equations with respect to $W_n$:

$$\sum_{n=1}^{N} \{h_k(x_n) w_n\} W_n = \frac{\partial H_k(m;\lambda)}{\partial \lambda}. \tag{A.20}$$

The solution of the problem

$$\min_{W_n} \frac{1}{2} \sum_{n=1}^{N} W_n^2 \tag{A.21}$$

which satisfies Eq. (A.20) does not change the parametric derivatives $\partial H_k/\partial\lambda$ of the first $K$ moments and reduces the scatter of the factors $W_n$.

Finally, the algorithm for calculation of the parametric derivatives is as follows. We simulate the coagulation process according to Eqs. (A.6) - (A.9) and recalculate $W_n$ according to Eqs. (A.16) - (A.19). When the scatter of the factors $W_n$ becomes too high we solve the problem (A.20) - (A.21). Since we do not need an exact minimum of (A.21), $2-4$ iterations of a projective gradient method are enough to stabilize the computations. Note that this procedure is not time-consuming and the required CPU time scales almost linearly with the number of the preserved moments $K$. The computational experiments with $K$ spans from 6 to 24 give very close results. All the results presented in this work are obtained with $K = 16$.

# References


[1] O.M. Alifanov, E.A. Artyukhin, and S.V. Rumyantsev. *Extreme Methods for Solving Ill-Posed Problems with Applications to Inverse Problems.* Begell House, 1995.

[2] G. K. Batchelor. *The theory of homogeneous turbulence.* Cambridge University Press, 1956.

[3] D. Colella, D. Vinci, R. Bagatin, M. Masi, and E.A Bakr. A study on coalescence and breakage mechanisms in three different bubble columns. *Chemical Engineering Sci.*, 54(21):4767 – 4777, 1999.

[4] C. A. Coulaloglou and C. Tsouris. Description of interaction processes in agitated liquid-liquid dispersions. *Chemical Engineering Sci.*, 32:1289 – 1297, 1977.

[5] A. Eibeck and W. Wagner. Stochastic particle approximation for Smoluchovski's coagulation equation. *Ann. Appl. Probab.*, 11:1137–1165, 2001.

[6] J.S. Ghalehchian and M.J. Slater. A possible approach to improving rotating disc contactor design accounting for drop breakage and mass transfer with contamination. *Chem. Eng. J.*, 75:131 – 144, 1999.

[7] J.C. Godfrey and M.J. Slater. Slip velocity relationships for liquidliquid extraction columns. *Trans. I. Chem. E.*, 69:130 – 141, 1991.

[8] M. Goodson and M. Kraft. Simulation of coalescence and breakage: an assessment of two stochastic methods suitable for simulating liquidliquid extraction. *Chemical Engineering Sci.*, 59:3865 – 3881, 2004.

[9] M. J. Hounslow and X. Ni. Population balance modelling of droplet coalescence and break-up in an oscillatory baffled reactor. *Chemical Engineering Sci.*, 59:819 – 828, 2004.

[10] T. Misek, R. Berger, and J. Schröter. *European Federation of Chemical Engineering: Standard Test Systems for Liquid Extraction.* The Institution of Chemical Engineers, 1985.

[11] G. Modes. *Grundsätzliche Studie zur Populationsdynamik einer Extraktionskolonne auf Basis von Einzeltropfenuntersuchungen.* PhD thesis, Universität Kaiserslautern, 1999.

[12] X. Ni, D. Mignard, B. Saye, J. C. Johnstone, and N. Pereira. On the evaluation of droplet breakage and coalescence rates in oscillatory baffled reactor. *Chemical Engineering Sci.*, 57:2101–2114, 2002.

[13] T. Pilhofer and H. D. Miller. Photoelektrische messmethode zur bestimmung der tropfengrenverteilung mitteldisperser tropfen in einem nichtmischbaren flssigen zweistoffsystem. *Chem. Ing. Tech.*, 44:295 – 300, 1972.

[14] D. Ramkrishna. *Population balances.* Academic press, 2000.

[15] D. Ramkrishna, A. Sathyagal, and G. Narishman. Analysis of dispersed-phase systems: fresh perspective. *AIChE Journal*, 41:35–44, 1995.

[16] C. P. Ribeiro(Jr). and P. L. C. Lage. Population balance modeling of bubble size distributions in a direct-contact evaporator using a sparger model. *Chemical Engineering Sci.*, 59(12):2363–2377, 2004.

[17] S. Rjasanow, T. Schreiber, and W. Wagner. Reduction of number of particles in the stochastic weighted method for the Boltzmann equation. *J. Comput. Phys.*, 145:382–405, 1998.

[18] M. Simon, S. A. Schmidt, and H.-J. Bart. The droplet population balance model - estimation of breakage and coalescence. *Chemical Engineering and Technol.*, 26:745 – 750, 2003.

[19] A. N. Tikhonov and V. Y. Arsenin. *Solution of ill-posed problems.* V. H. Winston and sons, 1977.

[20] C. Tsouris and L. L. Tavlarides. Breakage and coalescence model for drops in turbulaent dispersions. *AIChE Journal*, 49:395–406, 1994.

[21] A. Vikhansky and M. Kraft. Modeling of RDC using a combined CFD-population balance approach. *Chemical Engineering Sci.*, 59(13):2597 – 2606, 2004.

[22] A. Vikhansky and M. Kraft. A Monte Carlo methods for identification and sensitivity analysis of coagulation processes. *Journal of Computational Physics*, 200(1):50 – 59, 2004.